Three-dimensional hydrogen microscopy using a high-energy proton probe

G. Dollinger,[a] P. Reichart, G. Datzmann, A. Hauptner, and H.-J. Körner
Physik Department E12, Technische Universität München, 85748 Garching, Germany

(Received 4 September 2002; accepted 5 November 2002)

It is a challenge to measure two-dimensional or three-dimensional (3D) hydrogen profiles on a micrometer scale. Quantitative hydrogen analyses of micrometer resolution are demonstrated utilizing proton–proton scattering at a high-energy proton microprobe. It has more than an-order-of-magnitude better position resolution and in addition higher sensitivity than any other technique for 3D hydrogen analyses. This type of hydrogen imaging opens plenty room to characterize microstructured materials, and semiconductor devices or objects in microbiology. The first hydrogen image obtained with a 10 MeV proton microprobe shows the hydrogen distribution of the microcapillary system being present in the wing of a mayfly and demonstrates the potential of the method. © *2003 American Institute of Physics.* [DOI: 10.1063/1.1533111]

Hydrogen is an element which significantly influences the physical and chemical properties of any material. In a lot of materials like, e.g., organic matter it is one of the main constituents. However, even small fractions can have a strong influence on the properties of common metals, semiconductors, and insulators. Therefore, the quantitative analysis of hydrogen plays a crucial role in understanding the behavior and in improving the quality of materials.

Several techniques for quantitative hydrogen imaging have been developed.[1–6] However, imaging of hydrogen on a micrometer scale or even with resolutions better than a micrometer is a great challenge. Standard techniques for elemental analyses like x-ray fluorescence or Auger electron spectroscopy[7] are not applicable for hydrogen detection as a matter of principle. In addition, scattering cross sections for electrons and x rays are very low compared to any other element which hampers imaging of hydrogen by electron or x-ray microscopes. Hydrogen analysis using infrared spectroscopy[8] is restricted to a limited number of materials and a selection of hydrogen containing molecules. Considering secondary ion mass spectrometry as a destructive method for high resolution imaging near the surface, hydrogen microscopy is questionable due to the high mobility of the hydrogen atoms including unsolved problems regarding the quantification especially in materials like metals.[9] Other techniques which are commonly used for hydrogen imaging, like neutron radiography[3] or nuclear magnetic resonance microscopy[2] are limited in their resolving power to values of 10–100 μm and they are also restricted in terms of sensitivity.

These limits to analyze hydrogen in microscopic dimensions has been overcome now, since the scanning ion microprobe Superconducting Nanoscope for Applied nuclear (Kern-) physics Experiments (SNAKE) has gone into operation[10] which allows us to focus proton beams from 4 to 30 MeV to 1 μm in diameter. Elastic proton–proton scattering is utilized to obtain a quantitative and sensitive hydrogen analysis[11] at the actual position of the proton probe. Doing so at several positions a microscopic image of the hydrogen distribution is obtained. The details of this hydrogen microscopy will be described in the following.

SNAKE (Fig. 1) is a facility at the Munich 15 MV tandem accelerator which mainly consists of a two stage focusing system and several pairs of specially shaped slits[12] defining the phase space of the ion beam, e.g., a high-energy proton beam. The setup allows us to reduce beam size defined by the object slits by a factor of 200. A superconducting magnetic multipole lens[13] is used for the main (second) demagnification stage in order to focus high-energy ions within a short working distance from the lens of about 150 mm with minimized spherical aberrations. The overall position resolution has been checked with various grids to be at 1 μm. The resolution is actually limited by nonideal optics as well as from effects of vibrations and fluctuating electromagnetic fields on the stability of beam position.

Hydrogen detection is performed utilizing the elastic scattering of high-energy protons from hydrogen nuclei which are situated in the target. Since protons are also scattered from other elements in the target, a sensitive selection of the proton–proton scattering events is required for hydrogen analyses. A clear cut without ambiguity for these proton–proton scattering events is set by demanding coincident detection of the two protons emitted under a relative angle of 90° within the scattering plane.[11] A large area silicon strip detector (Fig. 2) is used for particle detection which covers a significant part (2.3 sr) of the total solid angle in order to detect nearly all of the valuable proton–proton scattering events. It gives an energy signal for each detected particle and a nanosecond coincidence window. In addition, the relative scattering angle of 90° in a scattering plane can be checked for two particles detected in coincidence due to the granularity of the detector. This redundant discrimination for proton–proton scattering events reduces background below 10^{-6} even at high count rates (e.g., 10 kHz), which are necessary for acceptable measurement times even at low hydrogen concentrations.

Thus, a sensitivity in the range of parts per million hydrogen atoms is obtained.[11,14] The number of detected proton–proton events is directly proportional to the areal density of hydrogen at the beam spot for a given beam dose.

[a]Electronic mail: guenther.dollinger@ph.tum.de

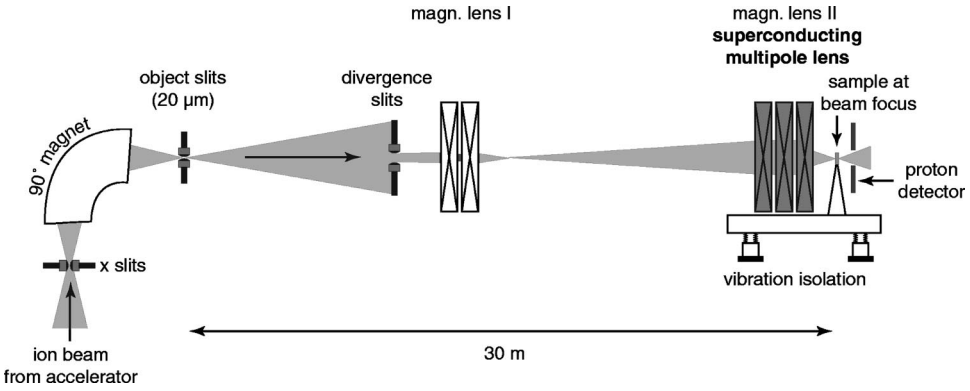

FIG. 1. Schematic drawing of the scanning ion microscope SNAKE at the Munich tandem accelerator. The object slit defines an already microscopic aperture which is demagnified 200 times by the two stage magnetooptical system. It allows a beam spot size of 100 nm with reasonable object aperture sizes of 20 μm.

A two-dimensional (2D) lateral hydrogen image of the target material is obtained by scanning the focused proton beam across the sample and by marking every proton–proton signal in a map at a position which corresponds to the actual beam position. The scanning of the beam is performed by electrostatic deflection plates driven step by step at a constant step rate of, e.g., 100 Hz. The minimum step size is adjusted to the beam size and can be in the nanometer range in principle.

The information on the third dimension, respectively, the depth of the hydrogen location, is obtained simultaneously for each detected event. For this purpose the sum of the kinetic energy of the two protons is measured. The incident and the scattered protons sustain an energy loss which increases with probing depth. Because energy loss of the scattered protons is larger than that of the incident protons a net effect remains for protons scattered in different depths. The achievable depth resolution was found to be better than 5 μm even at probing depths of some 100 μm.[15]

This method, commonly called ''proton–proton scattering,'' has already been used as a technique for hydrogen

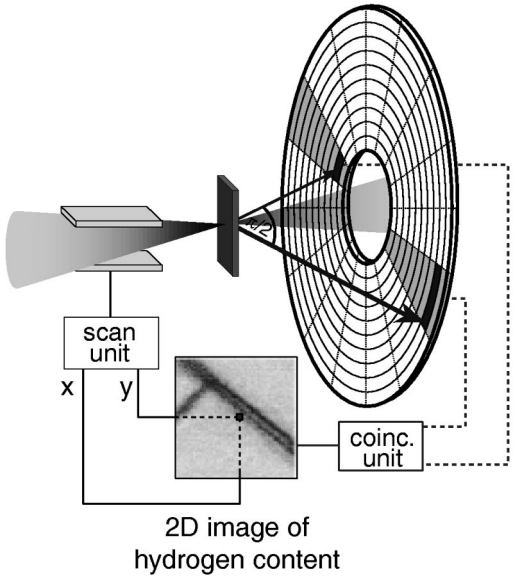

FIG. 2. Principle drawing of hydrogen analysis by proton–proton scattering. The two protons emitted from a proton scattered at a hydrogen nuclei of the sample are detected in coincidence by an annular silicon strip detector with huge solid angle of detection (2.3 sr). A small coincidence window in the nanosecond range and a subdivision in sectors and annular strips allows a sensitive selection of the proton–proton scattering events from all other scattering events.

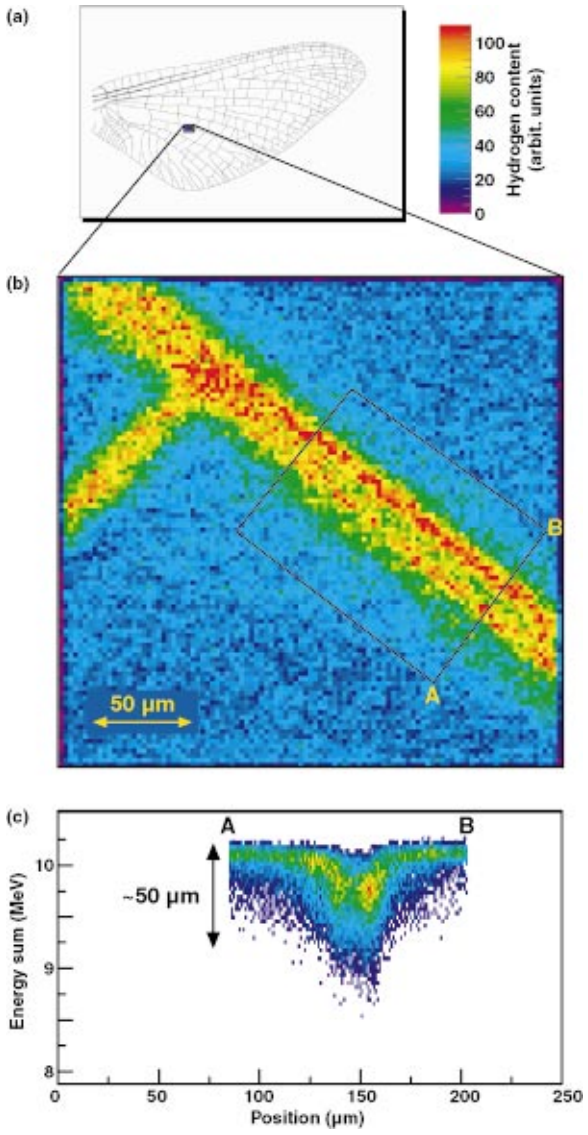

FIG. 3. (Color) (a) Schematic drawing of the wing of a mayfly (see Ref. 20). (b) 2D map of the hydrogen content of the wing from the marked region of Fig. 3(a). The supporting capillary system at a *T* junction can be recognized. The two-fold maximum at the main capillary results from the projection of the hollow tube. (c) Hydrogen cross-sectional profile of the marked area of Fig. 3(b) projected onto the base line AB. The third dimension is evaluated from the energy profile. The corresponding scale is plotted in the figure. The picture reveals the cross section of the capillary. However, the empty space in the tube is not imaged, because energy loss occurs only at the capillary wall, but not inside.

analyses at low-energy proton microprobes.[16] The major drawback of using low-energy protons was a limited range of the scattered protons. This restricted the analyses to a sample thickness in the 10 μm range since at least one of the two scattered protons has to be transmitted through the sample in order to get a true hydrogen signal. The limit is now significantly repelled by SNAKE whose high proton energies allow hydrogen microscopy with specimen of several 100 μm thickness. Therefore, nearly any material can be investigated with simple preparation schemes. The main strength of the proton–proton scattering is the large scattering cross section which results from the dominant strong nuclear interaction. It is nearly constant for scattering angles between 30° and 60° (e.g., $\sigma_{\mathrm{lab}} \approx 0.1 \times 10^{-24}$ cm^2/sr in the laboratory system for 19.8 MeV protons)[17] and about three orders of magnitude enhanced over the scattering cross section which would be expected from a pure Coulomb interaction. It has therefore by far the largest ratio of detection cross section to damage cross section of all other possible ion beam techniques for hydrogen analyses like elastic recoil detection[4,5,18] or nuclear reaction analysis.[19] Thus, it is the only technique which guarantees low enough beam damage that hydrogen images of submicron resolution can be gained without significantly changing the hydrogen content in the investigated area.[15]

In order to demonstrate the potential of the method, hydrogen distributions of a mayfly's wing (Ephomeroptera Heptageniidae) are shown in Figs. 3(b) and 3(c). The wing was dried and mounted without any further preparation at the target position of SNAKE. Figure 3(b) shows the hydrogen image from proton–proton scattering scanning a focused 10 MeV proton beam at 2.6 μm step size across the rectangular area marked in the principal drawing of the wing in Fig. 3(a).[20] A branching point of the capillary supply and support system of the wing which lies within the investigated area can clearly be recognized in this hydrogen image. The image directly shows the hydrogen content of the massive parts of the dried wing. The double peak structure seen at the main capillary results from the characteristic projected image of a hollow tube.

The third dimension of the hydrogen distribution was recorded simultaneously with the 2D map of Fig. 3(b). A cross section of the hydrogen distribution of the capillary is shown in Fig. 3(c). It is obtained by evaluating the sum energy spectrum of the detected proton pairs at each position of the base line AB where the pixels of the marked area in Fig. 3(b) are projected onto. The energy loss spectrum was transformed into a depth scale using tabulated values of stopping forces[21] for the relevant proton energies.

In summary, proton–proton scattering at a high-energy proton microprobe allows a quantitative three-dimensional hydrogen microscopy with a position resolution in the range of one micrometer and a sensitivity in the ppm region. The analysis can be extended by a simultaneously performed 2D mapping of other elements, e.g., using particle Induced x-ray emission[22] PIXE for the analysis of heavy elements. The high proton energies available at SNAKE allow investigation of unsupported samples of some 100 μm thickness and make an attractive step forward in the investigation of hydrogen containing microstructures, e.g., in microelectronics, micromechanics, geology, or even in biology. Completely new applications are expected for the microscopy of biological materials, e.g., interfaces between biologic and biocompatible materials, which can be investigated under living conditions in foil containers.

This work is supported by the Maier-Leibnitz-Laboratorium der Universität und der Technischen Universität München as well as the Bundesministerium für Bildung und Forschung.

[1] P. C. Lauterbur, Nature (London) **242**, 190 (1973).
[2] S. J. Blackband, D. L. Buckley, J. D. Bui, and M. I. Phillips, Magn. Reson. Mater. Phys., Biol., Med. **9**, 112 (1999).
[3] B. Schillinger, E. Lehmann, and P. Vontobel, Physica B **276–278**, 59 (2000).
[4] J. Tirira, P. Trocellier, J. P. Frontier, Ph. Massiot, J. M. Costantini, and V. Mori, Nucl. Instrum. Methods Phys. Res. B **50**, 135 (1990).
[5] B. P. Doyle, R. D. Maclear, S. H. Connell, P. Formenti, I. Z. Machi, J. E. Butler, P. Schaaff, J. P. F. Sellschop, E. Sideras-Haddad, and K. Bharuth-Ram, Nucl. Instrum. Methods Phys. Res. B **130**, 204 (1997).
[6] C. L. Churms, V. M. Prozesky, T. K. Marias, R. Pretorius, W. F. van-der-Weg, and W. Sinke, AIP Conf. Proc. **392**, 719 (1997).
[7] H. Hantsche, Scanning **11**, 257 (1989).
[8] B. C. Smith, *Fundamentals of Fourier Transform Infrared Spectrocopy* (CRC, Boca Raton, 1996).
[9] M. Riedel and H. Düsterhöft, Rapid Commun. Mass Spectrom. **12**, 1510 (1998).
[10] G. Datzmann, G. Dollinger, C. Goeden, A. Hauptner, H.-J. Körner, P. Reichart, and O. Schmelmer, Nucl. Instrum. Methods Phys. Res. B **181**, 20 (2001).
[11] B. L. Cohen, C. L. Fink, and J. H. Degnan, J. Appl. Phys. **43**, 19 (1972).
[12] O. Schmelmer, G. Dollinger, G. Datzmann, C. Goeden, and H.-J. Körner, Nucl. Instrum. Methods Phys. Res. B **158**, 107 (1999).
[13] G. Datzmann, G. Dollinger, G. Hinderer, and H.-J. Körner, Nucl. Instrum. Methods Phys. Res. B **158**, 74 (1999).
[14] B. G. Martinsson and P. Kristiansson, Nucl. Instrum. Methods Phys. Res. B **82**, 589 (1993).
[15] P. Reichart, G. Dollinger, A. Bergmaier, G. Datzmann, A. Hauptner, and H.-J. Körner, Nucl. Instrum. Methods Phys. Res. B **197**, 134 (2002).
[16] K. A. Sjöland, P. Kristiansson, M. Elfman, K. G. Malmqvist, J. Pallon, R. J. Utui, and C. Yang, Nucl. Instrum. Methods Phys. Res. B **124**, 639 (1997).
[17] J. W. Burkig, J. R. Richardson, and G. E. Schrank, Phys. Rev. **113**, 290 (1959).
[18] D. Grambole, F. Herrmann, R. Behrisch, and W. Hauffe, Nucl. Instrum. Methods Phys. Res. B **158**, 647 (1999).
[19] W. A. Landford, Nucl. Instrum. Methods Phys. Res. B **66**, 65 (1992).
[20] With permission of J. Gaul (http://home.knuut.de/juergen.gaul/).
[21] J. Ziegler, J. Biersack, and U. Littmark, *The Stopping and Range of Ions in Matter* (Pergamon, New York, 1985).
[22] O. Schmelmer, G. Dollinger, G. Datzmann, A. Hauptner, H.-J. Körner, P. Maier-Komor, and P. Reichart, Nucl. Instrum. Methods Phys. Res. B **179**, 469 (2001).